Many studies have demonstrated that basic fibroblast growth factor (bFGF) is one of the most potent of the various growth factors for cartilage repair (2–6). In order to establish an efficient approach for the treatment of cartilage defects, it may be advantageous to maintain a certain level of growth factor locally for a long time.

A new therapeutic approach to cartilage repair, gene therapy, has been described, in which genes are transduced into chondrocytes with the use of naked DNA or viral vectors (7–10). However, problems with this method are related to the ability to obtain high-efficiency transduction, to maintain long-term expression of the therapeutic gene, and safety. Recently, the adeno-associated virus (AAV) has been recognized as a tool for transducing a gene into target cells (11–14). Gene therapy with AAV has several advantages, including the lack of virulence of the wild-type virus, the safety, since there is no replication activity alone, the ability to transduce to nondividing cells, the integration into the host genome, and the long-term expression of the transduced gene.

In this study, we attempted to use this new delivery vector to repair cartilage defects, in an ex vivo method. The purpose of this study was to evaluate the utility of the AAV vector for ex vivo gene delivery to chondrocytes and to investigate the repair of an articular cartilage defect by transplantation of bFGF gene–transduced chondrocytes.

MATERIALS AND METHODS

AAV vector production. Two AAV constructs were prepared for this study: AAV-LacZ contained the bacterial β-galactosidase (LacZ) gene and AAV-bFGF contained the bFGF gene, which harbors a nuclear localization signal under the regulation of the cytomegalovirus immediate early promoter. The AAV subtype 2 vector plasmid used in this study, pLacZ, was derived from the vector plasmid pW1, which contains the LacZ gene, as previously described (15). Recombinant bFGF gene (GenBank accession no. X07285) was obtained from Takeda Chemical Industries (Osaka, Japan). A fragment containing bFGF complementary DNA was amplified by polymerase chain reaction using the following primer pairs with the *Eco* RI or the *Xho* I site: 5′-ATGAATTCATGGCTGCCGGCAGCATCACTTCGCTT-3′ and 5′-ATCTCGAGAGAGTCAGCTCTTAGCAGAC-3′. The fragment was subcloned between the *Eco* RI and *Xho* I sites of the pLacZ AAV vector plasmid to replace the LacZ gene (pbFGF). An AAV helper plasmid containing subtype 2 AAV *rep* and *cap* genes, which are required for replication and capsid formation of AAV vectors, pIM45 was used. A plasmid containing the E2A, E4, and VA genes of the adenovirus genome, pladeno-1, was used in place of helper adenovirus for AAV vector production.

Subconfluent human fetal kidney cells (293 cells) were cotransfected by the calcium phosphate coprecipitation method with pbFGF, pIM45, and pladeno-1 to produce the AAV-inducing bFGF gene (AAV-bFGF). After 48 hours, the cells were harvested and lysed in Tris HCl buffer (10 m*M* Tris HCl, 150 m*M* NaCl, pH 8.0) through 3 cycles of freezing and thawing. One round of sucrose precipitation and 2 rounds of CsCl density-gradient ultracentrifugation were performed to isolate AAV-bFGF from the lysates. The vector titer was determined by quantitative DNA dot-blot hybridization of the DNase I–resistant fraction.

Isolation of chondrocytes. Thirty-nine 10-week-old Japanese white rabbits (Oriental Yeast Company, Tokyo, Japan), weighing an average of 1.8 kg, were used in this study. They were divided into 3 groups: 9 for the LacZ-transduced group, 12 for the bFGF-transduced group, and 18 for the control group. Under intravenous anesthesia with pentobarbital sodium (Somnopentyl; Schering-Plough, Union, NJ), articular cartilage tissues (4 × 4–mm slices) were harvested from the patellar groove of the right knee, washed 3 times in phosphate buffered saline (PBS), and cut into small pieces. The pieces were treated with 0.05% trypsin and 0.001*M* EDTA (Gibco BRL, Gaithersburg, MD) for 30 minutes at 37°C and digested sequentially with 0.25% collagenase (type II collagenase; Worthington, Lakewood, NJ) for 3 hours at 37°C. The isolated chondrocytes were washed 3 times with PBS.

The mean number of cells collected from each rabbit was 2.4×10^5 (SD 0.5×10^5). These cells were divided into 4–6 culture wells and cultured in 24-well flat-bottomed plates (Falcon, Lincoln Park, NJ) at a concentration of 5×10^4 cells/well in 0.5 ml of Dulbecco's modified Eagle's medium (DMEM; Sigma, St. Louis, MO) supplemented with 10% fetal calf serum (FCS) and antibiotics (100 units/ml of penicillin G, 0.1 mg/ml of streptomycin; Gibco BRL) (DMEM–FCS), at 37°C in an atmosphere of 5% CO_2 in air.

Gene transduction into chondrocytes. Chondrocytes were cultured for 3 days, removed from the growth medium, and washed once with serum-free medium. To the culture wells for the transduced group was added 500 μl of serum-free DMEM containing AAV-LacZ or AAV-bFGF to enable quantification of transgene expression at the optimal number of viral particles (10^5 particles per cell) determined from the LacZ gene group experiments. To culture wells for the control group was added 500 μl of serum-free DMEM containing Tris buffer alone. After incubation for 1 hour at 37°C, 500 μl of DMEM–FCS was added to each culture well for both culture groups. One sample from each rabbit was used for autologous transplantation. The remaining samples were used for in vitro experiments.

Twenty samples from the LacZ-transduced group and 20 from the control group were used for the experiment to determine the efficacy of gene transduction in vitro. Culture medium was exchanged twice a week after gene transduction up to the time of analysis. At 3, 7, 14, 28, and 56 days after transduction, LacZ expression was assessed using the X-Gal staining technique (16), as follows. Cells were washed 3 times with PBS and fixed with 0.5% glutaraldehyde for 10 minutes, followed by 2 rinses in PBS containing 1 mmole/liter of $MgCl_2$. The cells were finally incubated with X-Gal substrate (1 mg/ml of X-Gal, 1 mmole/liter of $MgCl_2$, 5 mmoles/liter of $K_4Fe[CN]_6/K_3Fe[CN]_6$ in PBS) for 12 hours at 37°C. Efficiency of gene transduction was calculated as the average percentage

of X-Gal–positive cells per total number of living cells in 3 randomly selected fields viewed with an optical microscope.

Measurement of bFGF concentration in culture medium. Samples from 12 rabbits in the bFGF-transduced group and from 12 rabbits in the control group were used for determinations of accumulated bFGF production in the culture supernatant. The culture medium was not changed at each sampling of either group. At 3, 7, and 14 days after transduction, culture supernatants were collected from every 4 bFGF-transduced or control group culture wells, respectively, and after centrifugation, were stored at –80°C until analyzed. The bFGF concentration in the culture supernatants was measured by enzyme-linked immunosorbent assay (ELISA) using a bFGF-specific ELISA kit (Quantikine; R&D Systems, Minneapolis, MN) according to the manufacturer's instructions.

Autologous transplantation of gene-transduced chondrocytes into an articular cartilage defect. Chondrocytes from the LacZ-transduced, bFGF-transduced, and control groups were cultured for 1 week after gene transduction, collected from the culture wells by trypsinization, and then centrifuged. The supernatant was removed, and chondrocytes were embedded in a 0.2% solution of type I collagen (Cellgen; Koken, Tokyo, Japan) at a density of 1×10^6/ml. For autologous transplantation, chondrocytes were suspended in the collagen gel by incubation at 37°C for 1 hour.

Rabbits were anesthetized with pentobarbital sodium, and the left hind leg of each rabbit was sterilized for surgery. A 3-cm medial parapatellar incision was made over the knee, and the patella was dislocated laterally. A full-thickness defect in the articular cartilage (5 mm in diameter; 3 mm deep) was made in the patellar groove using a hand drill. The collagen gel containing $\sim 7.5 \times 10^4$ autologous chondrocytes was transplanted into the full-thickness defect. A periosteal flap of $\sim 5 \times 5$ mm was harvested from the anteromedial surface of the tibia and sutured to the peripheral rim of the artificial defect with 5-0 nylon thread. The cambium layer of the periosteal flap was faced toward the joint space. The rabbits were allowed to move freely immediately after surgery.

Among the 39 rabbits, LacZ-transduced chondrocytes were transplanted into 9, bFGF-transduced chondrocytes into 12, and chondrocytes without gene transduction into the remaining 18.

Evaluation of LacZ expression at the site of transplantation. Rabbits from the LacZ-transduced (n = 3) and control (n = 2) groups were killed at 1, 2, and 4 weeks after transplantation. The specimens were harvested from the patellar groove, embedded in TissueTek OCT compound (Sakura Finetek USA, Torrance, CA), and immediately frozen in nitrogen liquid. The frozen specimens were sectioned into 20-μm slices with a cryotome (Coldtome CM-502; Sakura Seiki, Tokyo, Japan) and double-stained with X-Gal and hematoxylin and eosin (H&E).

Histologic evaluation of repair cartilage. Rabbits from the bFGF-transduced (n = 4) and control (n = 4) groups were killed at 4, 8, and 12 weeks after transplantation. The distal part of the femur was resected en bloc, fixed with 10% buffered formalin, and decalcified with a 0.5*M* EDTA solution. Sagittal sections were prepared and stained with H&E, toluidine blue, or Safranin O–fast green. The histologic features of each specimen were evaluated semiquantitatively using the histologic scoring system described by Wakitani et al (17). This system consists of 5 categories (cell morphology, matrix staining, surface regularity, cartilage thickness, and integration of donor with host) scored on a 0–14-point scale, where 0 = complete regeneration and 14 = no regeneration.

Statistical analysis. Data are expressed as the mean ± SD. The statistical significance of differences was calculated with the use of StatView software (version J-5.0; Abacus Concepts, Berkeley, CA). One-way analysis of variance and the Mann-Whitney U test were used for analyzing statistical significance. *P* values less than 0.05 were considered significant.

RESULTS

In vitro experiment. *Efficiency of gene transduction of chondrocytes.* The efficiency of gene transduction was determined for chondrocytes transfected with AAV-LacZ at 7 days after transduction. The mean ± SD percentage of LacZ-positive cells among the total number of living cells was 43.7 ± 8.8%, 62.4 ± 5.1%, 97.7 ± 0.6%, and 98.2 ± 1.5% at a vector dose of 10^3, 10^4, 10^5, and 10^6 particles/cell, respectively (Figure 1). The percentage of successfully transduced chondrocytes increased in a vector dose–dependent manner. A vector dose of $>10^6$ particles/cell did not improve the transduction rate. The optimal dose of virus that was required to achieve transduction of ~100% of the chondrocytes was determined to be 10^5 particles/cell.

LacZ gene expression was highly maintained until 56 days after gene transduction. The mean ± SD percentage of LacZ-positive cells was 69.4 ± 15.1%, 97.7 ± 0.6%, 97.2 ± 1.8%, 95.8 ± 2.9%, and 85.8 ± 6.2% at 3, 7, 14, 28, and 56 days after transduction, respectively (Figure 2). The greatest population of

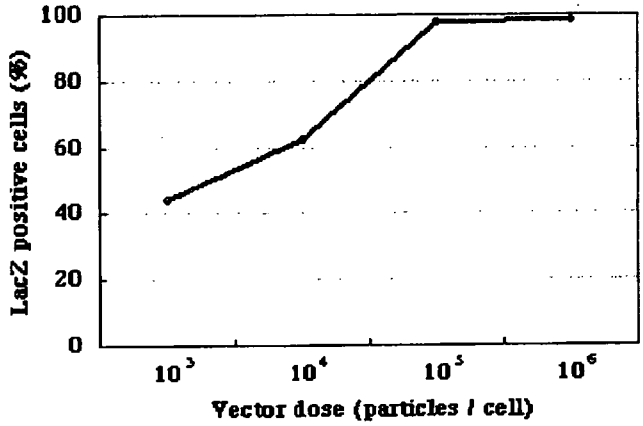

Figure 1. Vector dose–dependent LacZ expression in cultured chondrocytes. On day 7 after adeno-associated virus–LacZ transduction into chondrocytes, LacZ expression was assessed by X-Gal staining. The percentages of LacZ-positive cells among the total number of living cells were 43.7%, 62.4%, 97.7%, and 98.2% at doses of 10^3, 10^4, 10^5, and 10^6 particles/cell, respectively.

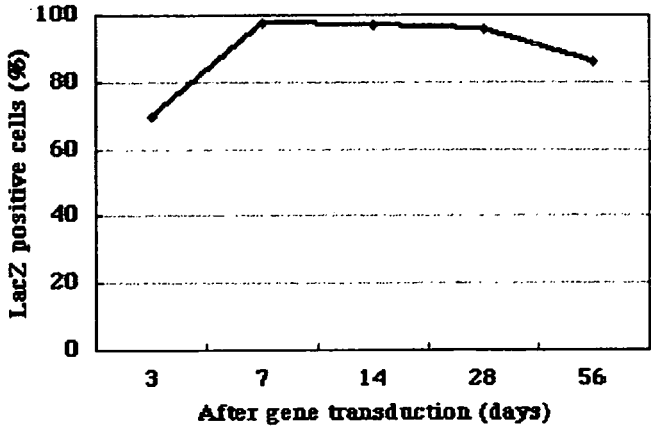

Figure 2. Time-dependent expression of LacZ in cultured chondrocytes. The percentages of LacZ-positive cells were 69.4%, 97.7%, 97.2%, 95.8%, and 85.8% at 3, 7, 14, 28, and 56 days after transduction, respectively.

LacZ-expressing cells was 97.7% at 7 days (Figure 3A), and more than 85% of the population was maintained up to 56 days. Cells without LacZ transduction in the control group failed to reveal LacZ expression at any sampling point (Figure 3B). There was no microscopic evidence of cell death or cytopathologic changes in the transduced cells as determined by optical microscopy.

Expression of bFGF gene by transduced chondrocytes. Production of bFGF was detected in both bFGF-transduced cells and control cells. The mean ± SD bFGF concentration in culture supernatants from the bFGF-transduced cells was 88.2 ± 9.8 ng/ml, 130.9 ± 28.8 ng/ml, and 240.6 ± 22.5 ng/ml at 3, 7, and 14 days after transduction, respectively (Figure 4). In control

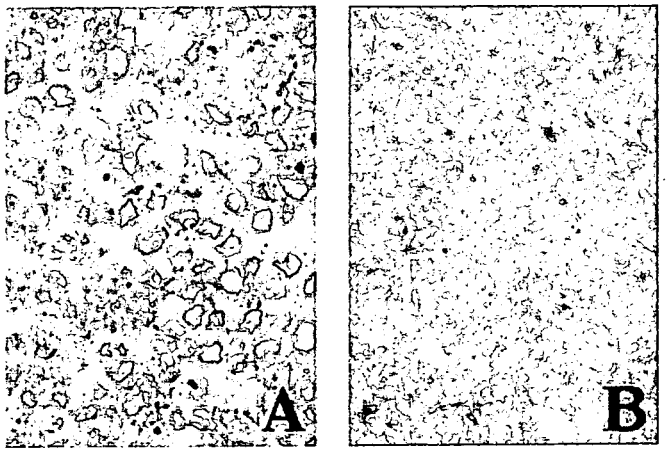

Figure 3. Photomicrographs of transduced chondrocytes stained with X-Gal. **A,** LacZ group chondrocytes were stained with X-Gal on day 7 after adeno-associated virus–LacZ transduction. LacZ-positive cells are stained blue. **B,** Control group chondrocytes showed no LacZ-positive cells. (Original magnification × 100.)

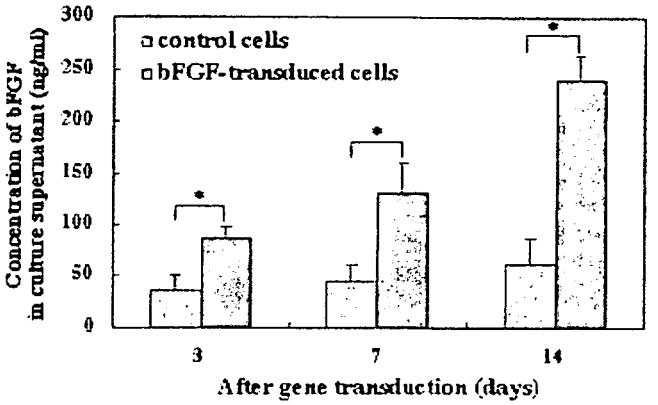

Figure 4. Concentration of basic fibroblast growth factor (bFGF) in culture supernatants of bFGF-transduced chondrocytes. Culture supernatants of control and bFGF-transduced cells were collected on days 3, 7, and 14 after transduction, and the bFGF concentration was determined by enzyme-linked immunosorbent assay. Transduction of the bFGF gene significantly elevated the secretion of bFGF (* = $P <$ 0.01).

cells, the bFGF concentration was 35.0 ± 15.8 ng/ml, 44.5 ± 16.4 ng/ml, and 62.3 ± 25.8 ng/ml at 3, 7, and 14 days after transduction, respectively. The bFGF concentration was significantly greater in bFGF-transduced cells than in the control cells on all sampling days ($P <$ 0.01).

The mean number of chondrocytes in the bFGF-transduced group was 14.1×10^4 (SD 1.1×10^4) and 34.8×10^4 (SD 6.2×10^4) at 7 and 14 days after transduction, respectively. In the control group, the numbers were 6.4×10^4 (SD 1.5×10^4) and 17.0×10^4 (SD 3.2×10^4) at 7 and 14 days after transduction, respectively. The mean number of chondrocytes in the bFGF-transduced group was significantly higher than that in the control group during the period of culture ($P < 0.01$).

In vivo experiment. *LacZ expression at the transplant site.* Throughout the observation period, X-Gal staining of LacZ-transduced cells showed cells with blue nuclei distributed across the entire regenerated cartilage under the layer covered by the transplanted periosteal flap. The controls, which received transplants without LacZ-transduced chondrocytes, did not show LacZ-positive cells at any week of sampling. No adverse effects related to the virus were observed in this ex vivo gene transfer experiment.

Macroscopic findings at the site of transplantation of the bFGF-transduced chondrocytes. Macroscopic observation of the transplant site showed regeneration of the articular cartilage defect in both the bFGF-transduced and control groups. At 12 weeks, the margin between the regenerated tissue and the

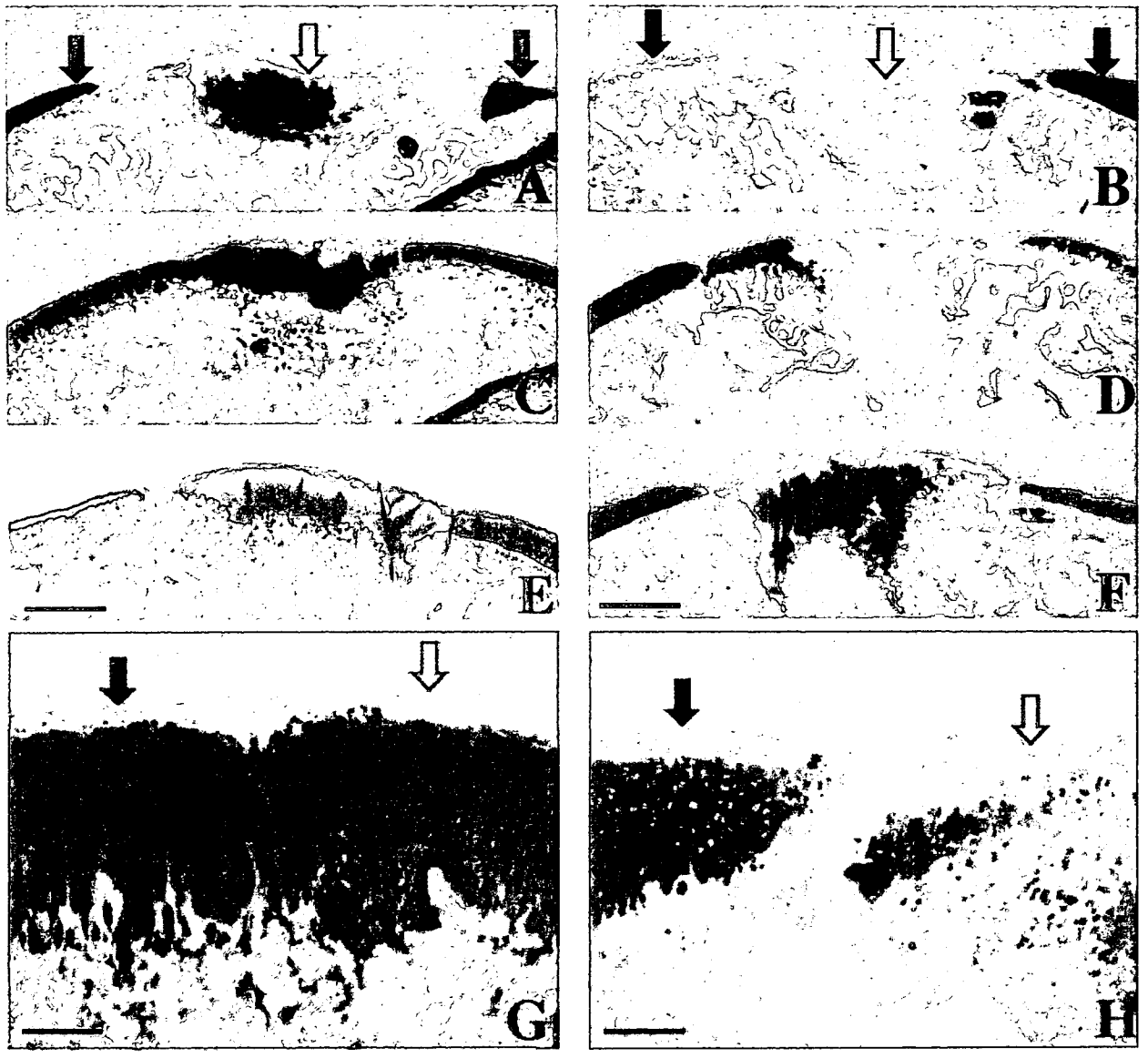

Figure 5. Photomicrographs of sagittal sections of articular cartilage defects in rabbits after transplantation with basic fibroblast growth factor (bFGF)–transduced chondrocytes (**A, C, E,** and **G**) and control chondrocytes (**B, D, F,** and **H**). Photomicrographs of the junction area are also shown (**G** and **F**). In the bFGF-transduced group, at 4 weeks (**A**), the deep layer is composed of round chondrocytes, but the matrix is weakly stained. At 8 weeks (**C**), the matrix is more distinctly stained, but the superficial region is weakly stained. At 12 weeks (**E** and **G**), the matrix is intensely metachromatically stained, and there is reconstitution of the osteochondral junction in most specimens. In the control group, at 4 weeks (**B**) and 8 weeks (**D**), the matrix is faintly stained. At 12 weeks (**F** and **H**), the deep layer of the matrix stained well, but staining is reduced in the superficial layers. **Solid arrows** indicate regenerated cartilage; **open arrows** indicate surrounding normal cartilage. Sections were stained with Safranin O–fast green. Bars in **A** and **F** = 1 mm; bars in **G** and **H** = 100 μm.

original cartilage was not distinguishable in both groups. The surface of the regenerated cartilage closely resembled normal cartilage in the bFGF-transduced group, but that in the control group could still be distinguished from surrounding normal cartilage. No sign of osteoarthrosis, such as erosion of cartilage or osteophyte formation, was seen in any of the knees during the observation period.

Histologic findings of regenerated cartilage following transplantation of bFGF-transduced chondrocytes. At 4 weeks after transplantation, in the tissues obtained from the bFGF-transduced group, the deep part of the

Table 1. Histologic scores of regenerated cartilage at 4, 8, and 12 weeks*

Weeks after transplantation	Control group	bFGF-transduced group
4	8.8 ± 1.0	6.5 ± 0.6†
8	7.0 ± 1.4	4.3 ± 1.0†
12	5.5 ± 1.7	2.8 ± 1.0†

* The histologic features were scored on a 0–14-point scale as described by Wakitani et al (17), where 0 represents complete regeneration and 14 represents no regeneration. Values are the mean ± SD. bFGF = basic fibroblast growth factor.
† $P < 0.01$ versus controls.

regenerated tissue was composed of round chondrocytes, with an extracellular matrix that stained weakly with Safranin O (Figure 5A). There was no integration of the edges of the regenerated tissue with the adjacent normal cartilage or reconstitution of the osteochondral junction in any specimen. In the control group, the extracellular matrix was faintly stained with Safranin O (Figure 5B).

At 8 weeks, the bFGF-transduced group showed an extracellular matrix that was more distinctly stained with Safranin O in the deep part, while the superficial part was weakly stained (Figure 5C). Although both edges were integrated with the adjacent normal cartilage, reconstitution of the osteochondral junction was not seen in any specimen. The tissues from the control group at 8 weeks were essentially the same as those at 4 weeks (Figure 5D).

In the bFGF-transduced group at 12 weeks, the intensity and thickness of the extracellular matrix that was metachromatically stained with Safranin O were increased as compared with the findings at 4 and 8 weeks, and the microstructure of the regenerated tissue resembled the surrounding normal cartilage (Figures 5E and G). There was reconstitution of the osteochondral junction in most of the specimens. In the control group, the deep layer of the regenerated cartilage matrix stained well with Safranin O, but staining was reduced in the superficial layers (Figures 5F and H). There was no reconstitution of the osteochondral junction in any of the control specimens.

The Wakitani score was 6.5 ± 0.6, 4.3 ± 1.0, and 2.8 ± 1.0 points (mean ± SD) at 4, 8, and 12 weeks after transplantation, respectively, in the bFGF-transduced group. In the control group, the score was 8.8 ± 1.0, 7.0 ± 1.4, and 5.5 ± 1.7 points at 4, 8, and 12 weeks after transplantation, respectively (Table 1). The scores in both groups gradually decreased throughout the experimental period. However, the score in the bFGF-transduced group became significantly lower than that in the control group with the passage of time postoperatively ($P < 0.01$).

DISCUSSION

Autologous chondrocyte transplantation has been successfully applied in recent years to the treatment of focal cartilage defects in a series of patients (18). Autologous chondrocytes for grafting are harvested from non–weight-bearing areas, cultured in vitro, reinjected into the cartilage defect, and the area is covered with a periosteal flap that is sutured in place. However, this method may be limited to small local cartilage defects, since the number of cells collected from donor sites to be used for cultivation is still limited.

Augmentation of the procedure with bFGF for help in repairing the cartilage has been reported to be efficacious (4–6,19). Weisser et al (4) reported that among several different growth factors used to treat transplanted chondrocytes, positive effects on cartilage repair were observed only with the bFGF-treated chondrocyte implants (4). Previous studies showed that exogenous bFGF induces the proliferation of chondrocytes, the maturation of cartilage, and the differentiation of mesenchymal cells, and it stimulates the synthesis of cartilaginous matrix (5,6). Otsuka et al (19) reported that continuous administration of bFGF using an osmotic pump had a clearly beneficial effect on repair of cartilage defects. However, bFGF alone did not lead to complete structural restitution of hyaline cartilage to repair the full-thickness defects of articular cartilage. Prolonged local expression of bFGF by transduction of the genetic code of bFGF into chondrocytes would be an efficient treatment for articular cartilage defects.

For the repair of cartilage defects with gene therapy, it may be necessary to obtain high-efficiency transduction and continuous local expression of the therapeutic gene. Several studies have demonstrated that the AAV vector has the ability to highly efficiently transduce a gene into cells, to integrate into the host genome, and to express the transduced gene for a long time (20–22). There are studies of the utility of the AAV vector for joint disease that demonstrated high-efficiency gene delivery to the synovium in vivo (23) or gene transduction to cultured chondrocytes in vitro (24). Delivering genes directly to the surface of the abnormal articular cartilage in order to accelerate cartilage repair could result in a long-term treatment. The advantage of ex vivo gene delivery would be direct delivery of the therapeutic gene to the abnormal articular cartilage and the ability to limit the area of gene expression to the cartilage defect alone. In our previous study, ex vivo

gene transfer to periosteum-derived cells using an AAV vector induced LacZ expression for 4 weeks in vivo (25).

In this study, high-efficiency LacZ gene transduction into chondrocytes was obtained long-term in vitro, and LacZ gene expression in vivo was sustained without any adverse effects. These findings suggest that gene transfer to an articular cartilage defect by use of the ex vivo method was established with the AAV vector. Cartilage repair was slightly inferior to that described in previous reports, even though we used 10-week-old rabbits for the experiment. One of the reasons was thought to be differentiation to fibrous chondrocytes during the 1-week culture before transplantation. The cell number and the bFGF secretion were significantly increased in bFGF-transduced chondrocytes compared with the control chondrocytes in vitro. Furthermore, the histologic appearance of the transplant site in the bFGF-transduced group was fully repaired compared with that in the control group. The repair at a comparatively early stage was apparently different between bFGF-transduced and null chondrocytes even at 12 weeks. Continuous bFGF secretion by gene transfer seemed to be an effective way to promote cartilage repair.

These results demonstrate that repair of full-thickness defects in rabbit articular cartilage can be enhanced by transplantation of bFGF gene–transduced chondrocytes. This method seems to be one of the best techniques for achieving repair of articular cartilage defects.

ACKNOWLEDGMENT

We thank Avigen, Inc. (Alameda, CA) for supplying the plasmid for the production of the AAV vector.

REFERENCES

1. Brittberg M, Lindahl A, Nilsson A, Ohlsson C, Isaksson O, Peterson L. Treatment of deep cartilage defects in the knee with autologous chondrocyte transplantation. N Engl J Med 1994;331: 889–95.
2. Kato Y, Gospodarowicz D. Sulfated proteoglycan synthesis by confluent cultures of rabbit costal chondrocytes grown in the presence of fibroblast growth factor. J Cell Biol 1985;100:477–85.
3. Hunziker EB, Rosenberg LC. Repair of partial-thickness defects in articular cartilage: cell recruitment from the synovial membrane. J Bone Joint Surg Am 1996;78:721–33.
4. Weisser J, Rahfoth B, Timmermann A, Aigner T, Brauer R, von der Mark K. Role of growth factors in rabbit articular cartilage repair by chondrocytes in agarose. Osteoarthritis Cartilage 2001; 9:48–54.
5. Shida J, Jingushi S, Izumi T, Iwaki A, Sugioka Y. Basic fibroblast growth factor stimulates articular cartilage enlargement in young rats in vivo. J Orthop Res 1996;14:265–72.
6. Cuevas P, Burgos J, Baird A. Basic fibroblast growth factor (FGF) promotes cartilage repair in vivo. Biochem Biophys Res Commun 1988;156:611–8.
7. Arai Y, Kubo T, Kobayashi K, Takeshita K, Takahashi K, Ikeda T, et al. Adenovirus vector-mediated gene transduction to chondrocytes: in vitro evaluation of therapeutic efficiency of transforming growth factor-β1 and heat shock protein 70 gene transduction. J Rheumatol 1997;24:1787–95.
8. Baragi VM, Renkiewicz RR, Qiu L, Brammer D, Riley JM, Sigler RE, et al. Transplantation of adenovirally transduced allogeneic chondrocytes into articular cartilage defects in vivo. Osteoarthritis Cartilage 1997;5:275–82.
9. Doherty PJ, Zhang H, Tremblay L, Manolopoulos V, Marshall KW. Resurfacing of articular cartilage explants with genetically-modified human chondrocytes in vitro. Osteoarthritis Cartilage 1998;6:153–9.
10. Kang BR, Marui T, Ghivizzani SC, Nita IM, Georgescu HI, Suh JK, et al. Ex vivo gene transfer to chondrocytes in full-thickness articular cartilage defects: a feasibility study. Osteoarthritis Cartilage 1997;5:139–43.
11. Schwarz EM. The adeno-associated virus vector for orthopaedic gene therapy [review]. Clin Orthop 2000;379 Suppl:S31–9.
12. Kaplitt MG, Leone P, Samulski RJ, Xiao X, Pfaff DW, O'Malley KL, et al. Long-term gene expression and phenotypic correction using adeno-associated virus vectors in the mammalian brain. Nat Genet 1994;8:148–54.
13. Xiao X, Li J, McCown TJ, Samulski RJ. Gene transfer by adeno-associated virus vectors into the central nervous system. Exp Neurol 1997;144:113–24.
14. Berns KI, Giraud C. Adenovirus and adeno-associated virus as vectors for gene therapy. Ann N Y Acad Sci 1995;772:95–104.
15. Xin KQ, Urabe M, Yang J, Nomiyama K, Mizukami H, Hamajima K, et al. A novel recombinant adeno-associated virus vaccine induces a long-term humoral immune response to HIV. Hum Gene Ther 2001;12:1047–61.
16. Price J, Turner D, Cepko C. Lineage analysis in the vertebrate nervous system by retrovirus-mediated gene transfer. Proc Natl Acad Sci U S A 1987;84:156–60.
17. Wakitani S, Goto T, Pineda SJ, Young RG, Mansour JM, Caplan AI, et al. Mesenchymal cell-based repair of large, full-thickness defects of articular cartilage. J Bone Joint Surg Am 1994;76: 579–92.
18. Richardson JB, Caterson B, Evans EH, Ashton BA, Roberts S. Repair of human articular cartilage after implantation of autologous chondrocytes. J Bone Joint Surg Br 1999;81:1064–8.
19. Otsuka Y, Mizuta H, Takagi K, Iyama K, Yoshitake Y, Nishikawa K. Requirement of fibroblast growth factor signaling for regeneration of epiphyseal morphology in rabbit full-thickness defects of articular cartilage. Dev Growth Differ 1997;39:143–56.
20. Kessler PD, Podsakoff GM, Chen X, McQuiston SA, Colosi PC, Matelis LA, et al. Gene delivery to skeletal muscle results in sustained expression and systemic delivery of a therapeutic protein. Proc Natl Acad Sci U S A 1996;93:14082–7.
21. Fisher KJ, Jooss K, Alston J, Yang Y, Haecker SE, High K, et al. Recombinant adeno-associated virus for muscle directed gene therapy. Nat Med 1997;3:306–12.
22. Herzog RW, Hastrom JN, Kung SH, Tai SJ, Wilson JM, Fisher KJ, et al. Stable gene transfer and expression of human blood coagulation factor IX after intramuscular injection of recombinant adeno-associated virus. Proc Natl Acad Sci U S A 1997;94:5804–9.
23. Goater J, Muller R, Kollias G, Firestein GS, Sanz I, O'Keefe RJ, et al. Empirical advantages of adeno associated viral vectors for in vivo gene therapy for arthritis. J Rheumatol 2000;27:983–9.
24. Arai Y, Kubo T, Fushiki S, Mazda O, Nakai H, Iwaki Y, et al. Gene delivery to human chondrocytes by an adeno associated virus vector. J Rheumatol 2000;27:979–82.
25. Kobayashi N, Koshino T, Uesugi M, Yokoo N, Xin KQ, Okuda K, et al. Gene marking in adeno-associated virus vector infected periosteum-derived cells for cartilage repair. J Rheumatol 2002; 29:2176–80.

Available online at www.sciencedirect.com

ScienceDirect

Virology xx (2008) xxx–xxx

VIROLOGY

www.elsevier.com/locate/yviro

Antibody-dependent enhancement of adeno-associated virus infection of human monocytic cell lines

Seiichiro Mori, Takamasa Takeuchi, Tadahito Kanda *

Center for Pathogen Genomics, National Institute of Infectious Diseases, 1-23-1 Toyama, Shinjuku-ku, Tokyo 162-8640, Japan

Received 14 November 2007; returned to author for revision 4 January 2008; accepted 25 January 2008

Abstract

In host animals, adeno-associated virus (AAV) is detectable mainly in the lymphoid tissue, which appears to be a target in natural infection. We used the human monocytic cell lines THP-1 and U937 to study the effect of mouse anti-AAV2 antiserum on infection with an AAV2 vector having the luciferase gene (AAV2/Luc). AAV2/Luc was found to infect THP-1 and U937 cells much less efficiently than HeLa cells, as monitored with the induced enzyme activity. Pre-incubation of AAV2/Luc with anti-AAV2 antiserum at a sub-neutralizing concentration enhanced by 2-to-10 fold infection of THP-1 and U937 with AAV2/Luc, but not of HeLa. Similarly, anti-AAV10 serum at a low level enhanced infection of THP-1 with AAV10/Luc. Sera of two cynomolgus monkeys, which had been probably infected with an AAV2-like virus, enhanced infection of THP-1 with AAV2/Luc. The enhancement was reduced with blocking the IgG-receptors Fcγ-RI and Fcγ-RII, which were displayed on the surface of THP-1 and U937 but not HeLa cells, with anti-Fcγ-RI antibody or anti-Fcγ-RII antibody. The data indicate that infection of Fcγ receptor-bearing cells with AAV is enhanced by anti-AAV IgG antibodies at a sub-neutralizing concentration that play a role in linking AAV particles and Fcγ receptors.

Keywords: AAV; Anti-AAV antibody; ADE; Fcγ-receptor

Introduction

Adeno-associated virus (AAV) is a nonenveloped icosahedral particle (a diameter of 25 nm) containing a single-stranded linear DNA (4.7 kb). To date several AAV serotypes and over 100 AAV variants have been recorded (Wu et al., 2006). Among them AAV serotype type 2 (AAV2) has been studied most extensively and used for gene therapy trials. Efficient propagation of AAV2 in cultured cells requires coinfection with a helper virus (Carter et al., 1979; Richardson and Westphal, 1981; Buller et al., 1981; McPherson et al., 1985). Without a helper virus the AAV DNA is integrated into cell DNA at a specific site and maintained as a provirus (Phone [illegible]). When a latently infected cell is super-infected with adenovirus, the integrated AAV is induced to replicate ([illegible] Cheung et al., 1980). A low level induction has been observed upon Fas-mediated apoptosis of the latently infected cells (Mori et al., 2002).

The tissue tropism of AAV in natural infection is not fully elucidated. AAV10, AAV11, and AAVcy.7 have been detected mainly in the lymphoid tissue and ileum of the naturally infected cynomolgus monkeys (Mori et al., 2008). AAV2 vectors injected to monkeys are detectable in the lymphoid tissue (Conrad et al., 1996; Favre et al., 2001; Lai et al., 2002; Nathwani et al., 2002; Davidoff et al., 2005; Mori et al., 2006) and the leukocytes (Favre et al., 2001; Lai et al., 2002). These studies suggest that the leukocytes are one of the major targets for AAV.

Infection of the leukocytes with dengue virus (DENV) is enhanced by either sub-neutralizing level of serotype-specific anti-DENV antibody or cross-reactive anti-DENV antibody (Fujita et al., 1986). The antibody, which binds to the virion at its variable region and to the cell-surface Fcγ receptor (Fcγ-R) at its Fc-region, mediates attachment of the virion to the surface

* Corresponding author. Fax: +81 3 5285 1166.
E-mail address: kanda@nih.go.jp (T. Kanda).

0042-6822/$ - see front matter © 2008 Elsevier Inc. All rights reserved.
doi:10.1016/j.virol.2008.01.033

Please cite this article as: Mori, S., et al., Antibody-dependent enhancement of adeno-associated virus infection of human monocytic cell lines, Virology (2008), doi:10.1016/j.virol.2008.01.033

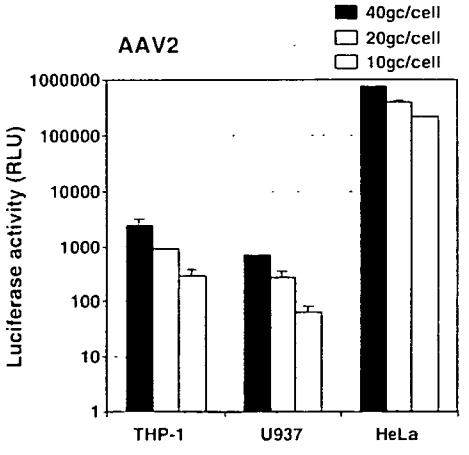

Fig. 1. Infection of THP-1, U937, and HeLa cells with AAV2/Luc. AAV2/Luc was inoculated to the cells at three multiplicities of infection (gc/cell). Two days later, the cells were lysed and luciferase activities of the lysates were measured. Each bar represents the average of three independent experiments with the standard deviation indicated by an error bar. RLU: relative light units.

of monocytes and macrophages (Clyde et al., 2006). This antibody-dependent enhancement (ADE) of DENV is believed to be associated with dengue hemorrhagic fever. Similar ADE has been reported in infection of Fcγ-R-positive cells with West Nile virus (Peiris and Porterfield, 1979; Peiris et al., 1981), human parvovirus B19 (Munakata et al., 2006), and Aleutian mink disease parvovirus (Kanno et al., 1993).

In this study we examined infection of THP-1 and U937, human monocytic cell lines that were expressing Fcγ-R, with recombinant AAV vectors that had been pre-incubated with diluted anti-AAV antiserum and found that a sub-neutralizing level of the antiserum enhanced infection of these cells with AAV vectors.

Results

Antibody-dependent-enhancement of infection of THP-1 and U937 cells with AAV2 and AAV10

Infection of THP-1 and U937, human monocytic cell lines, with AAV2/Luc, a recombinant AAV having the luciferase gene, was much less efficient than that of HeLa. Serially diluted AAV2/Luc was inoculated to the cells and 2 days later the cells were lysed and the luciferase activities of the lysates were measured (Fig. 1). While the luciferase activity of the HeLa culture inoculated with AAV2/Luc at a multiplicity of infection (MOI) of 10 genome copies (gc) was 200,000 U, those of the THP-1 and U937 cultures inoculated at an MOI of 40 gc were 2500 U and 1000 U, respectively.

Infection of THP-1 and U937 cells with AAV2/Luc was enhanced by pre-incubation of AAV2/Luc with a sub-neutralizing concentration of anti-AAV2 antiserum. AAV2/Luc was incubated with mouse anti-AAV2 antiserum or mouse normal serum at 37 °C for 30 min and then inoculated to 3×10^5 of THP-1 cells (at MOIs of 10, 20, and 40 gc), U937 cells (at MOIs of 50, 100, and 200 gc), and HeLa cells (at MOIs of 1, 2, and 4 gc). Two days later the luciferase activity of the cellular lysate was measured. The antiserum diluted at 1:100 induced a major decrease of the luciferase activities of the three cell lines, indicating that AAV2/Luc was neutralized with the antiserum (Figs. 2, A, B, and C). Although the antiserum diluted at 1:1000 induced a slight decrease of the luciferase activity of HeLa (Fig. 2C), it induced increase of the luciferase activities of THP-1 and of U937 (Figs. 2, A and B). The antiserum diluted at 1:10,000 and the normal mouse serum did not affect the luciferase activities of the three cell lines (Fig. 2). Thus, the antiserum diluted at 1:1000 enhanced infection of THP-1 and U937 with AAV2/Luc, indicating that typical ADE occurred in infection to these cells with AAV2.

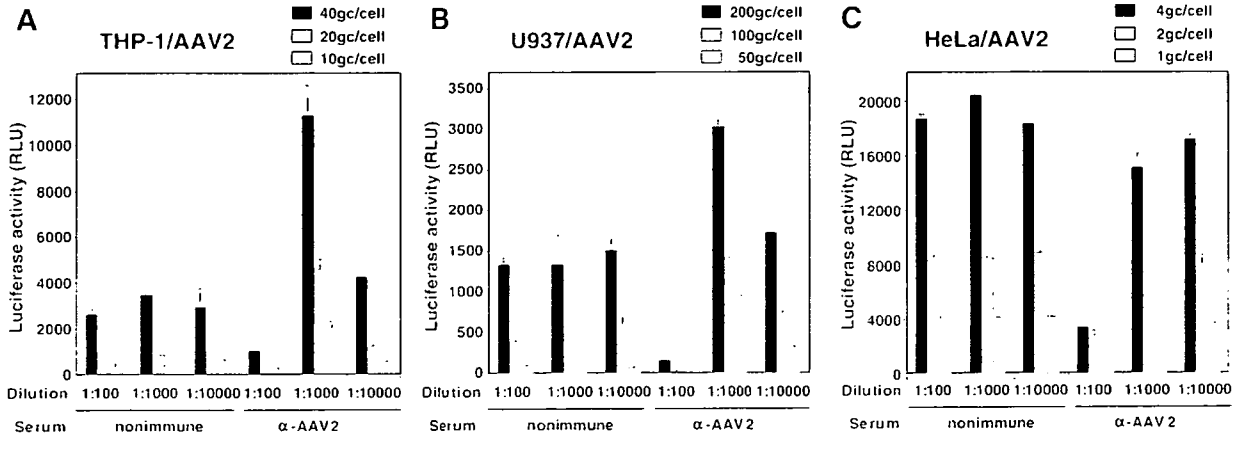

Fig. 2. Effect of anti-AAV2 antiserum on the infection of THP-1, U937, and HeLa cells with AAV2/Luc. AAV2/Luc was mixed with the diluted nonimmune serum or anti-AAV2 antiserum and incubated at 37 °C for 30 min. The mixtures were inoculated to THP-1 (A), U937 (B), or HeLa (C) cells at various multiplicities of infection (gc/cell) indicated. Two days later, the luciferase activity of the cellular lysate was measured. Each bar represents the average of three independent experiments with the standard deviation indicated by an error bar. RLU: relative light units.

Please cite this article as: Mori, S., et al., Antibody-dependent enhancement of adeno-associated virus infection of human monocytic cell lines. Virology (2008), doi:10.1016/j.virol.2008.01.033

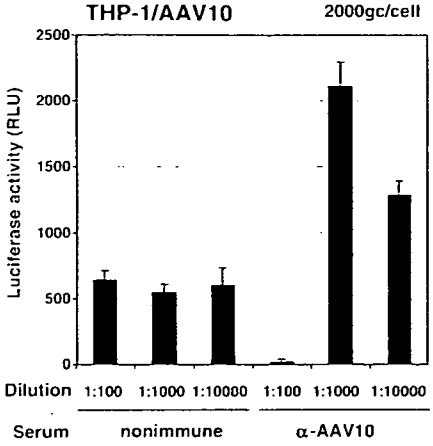

Fig. 3. Effect of anti-AAV10 antiserum on the infection of THP-1 cells with AAV10/Luc. AAV10/Luc was mixed with the diluted nonimmune serum or anti-AAV10 antiserum and incubated at 37 °C for 30 min. The mixtures were inoculated to THP-1 cells at the multiplicity of infection (gc/cell) indicated. Two days later, the luciferase activity of the cellular lysate was measured. Each bar represents the average of three independent experiments with the standard deviation indicated by an error bar. RLU: relative light units.

Similarly, infection of THP-1 cells with AAV10 was enhanced by a sub-neutralizing concentration of anti-AAV10 serum. AAV10/Luc pre-incubated with mouse anti-AAV10 serum was inoculated to THP-1 (3×10^5 cells) at an MOI of 2000 gc and the luciferase activity was measured as the experiments with AAV2/Luc. The antiserum reduced the infectivity of AAV10/Luc at a dilution of 1:100 but increased the infectivity at dilutions of 1:1000 and 1:10,000 (Fig. 3).

Anti-AAV2 and anti-AAV10 sera did not increase the infectivity of AAV10/Luc and AAV2/Luc, respectively (Fig. 4), indicating clearly that the antibody capable of binding to AAV particles mediates the enhancement of infection of THP-1 cells with AAV.

Two monkey sera enhanced infection of THP-1 cells with AAV2/Luc. Sera were obtained from two healthy male cynomolgus monkeys of 5 years of age. The pre-incubation of AAV2/Luc with the monkey-A serum that had been undiluted or diluted at 1:10 reduced the infectivity of AAV2/Luc to HeLa and to THP-1 (Figs. 5, A and B), indicating that the serum contained antibody capable of neutralizing AAV2. Pre-incubation of AAV2/Luc with the monkey-A serum that had been diluted at 1:100 and 1:1000 did not affect the infectivity to HeLa but it increased the infectivity to THP-1 (Figs. 5, A and B). Similarly, pre-incubation of AAV2/Luc with the undiluted monkey-B serum, which did not neutralize AAV2/Luc (Fig. 5A), enhanced infection of THP-1 (Fig. 5B). The data clearly indicate that monkey-B serum diluted at 1:10 and 1:100 did not affect the infectivity of AAV2/Luc (Fig. 5B). The data strongly suggest that the two monkeys had been probably infected with AAV types antigenically related to AAV2 and the sub-neutralizing levels of the antibodies in the sera enhanced infection of THP-1 with AAV2/Luc.

Involvement of the cell-surface Fcγ-receptors (Fcγ-R) in the ADE of AAV infection

Both Fcγ-RI and Fcγ-RII were present on the surface of THP-1 and U937 cells. THP-1, U937, and HeLa cells were incubated with anti-CD64 mouse monoclonal antibody (mAb) recognizing Fcγ-RI or anti-CD32 mouse mAb recognizing Fcγ-RII at 4 °C for 1 h. Then the mAb on the surface was detected with labeled-goat anti-mouse IgG antibody by using a FACS. Both mAbs clearly bound to the surface of THP-1 and U937 cells but did not bind to the surface of HeLa cells (Fig. 6).

Pretreatment of THP-1 and U937 with anti-CD64 mAb or anti-CD32 mAb interfered with ADE in the infection of these cells with AAV2/Luc. THP-1 and U937 cells were incubated with anti-CD64 mAb (5 μg/ml) and/or anti-CD32 (5 μg/ml) mAb at 4 °C for 1 h. The cells were inoculated with AAV2/Luc that had been pre-incubated with the anti-AAV2 antiserum diluted at 1:1000 and the luciferase activities of the lysates were measured at 2 days after the inoculation. The level of the enhancement of infection of both cell lines with AAV2/Luc was reduced by pretreatment with mAbs (Fig. 7), indicating that

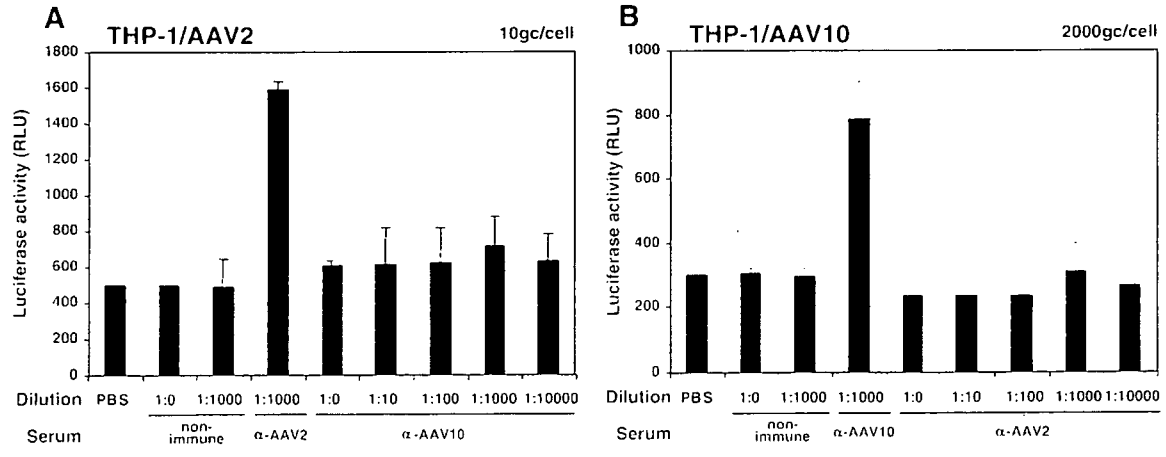

Fig. 4. Requirement of type-specific antibody for ADE of infection of THP-1 cells with AAV2/Luc and AAV10/Luc. AAV2/Luc (A) and AAV10/Luc (B) were pre-incubated with the undiluted or diluted anti-AAV2 or anti-AAV10 antiserum and inoculated to THP-1 cells. Two days later, the luciferase activity of the cellular lysate was measured. Each bar represents the average of three independent experiments with the standard deviation indicated by an error bar. RLU: relative light units.

Please cite this article as: Mori, S., et al., Antibody-dependent enhancement of adeno-associated virus infection of human monocytic cell lines, Virology (2008), doi:10.1016/j.virol.2008.01.033

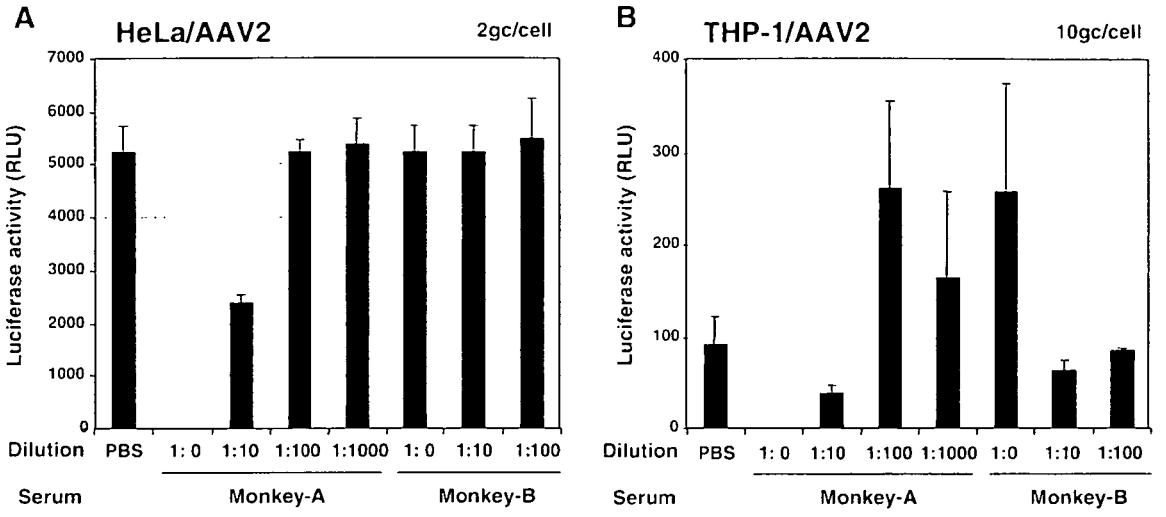

Fig. 5. Effect of the two monkey sera on the infection of THP-1 and HeLa cells with AAV2/Luc. AAV2/Luc was pre-incubated with the undiluted or the diluted cynomolgus monkey sera and inoculated to HeLa (A) or THP-1 (B) cells. Two days later, the luciferase activity of the cellular lysate was measured. Each bar represents the average of three independent experiments with the standard deviation indicated by an error bar. RLU: relative light units.

both Fcγ-RI and Fcγ-RII are involved in the enhancement. Anti-CD64 mAb was more effective than anti-CD32 mAb for the reduction and the mixture of anti-CD64 and anti-CD32 mAbs completely abolished the enhancement.

Discussion

We demonstrated that infection of THP-1 and U937, human monocytic cell lines, with AAV2/Luc was enhanced by the sub-neutralizing concentration of anti-AAV2 antibody. Similarly infection of THP-1 with AAV10/Luc was enhanced by the sub-neutralizing concentration of anti-AAV10 antibody. Cell-surface Fcγ-RI and Fcγ-RII were required for the enhancement, indicating that the antibodies play a role in linking the AAV particle and the Fcγ-R on the cell surface. A variety of leukocytes are positive for Fcγ-RI (monocytes/macrophages, dendritic cells, and neutrophils) and Fcγ-RII (monocytes/macrophages, dendritic cells, neutrophils, B lymphocytes, and mast cells)(Cohen-Solal et al., 2004). It is possible that infection of these cells with AAV is enhanced with a low level of anti-AAV antibodies in vivo.

The naturally infected AAV does not induce the strong immune response of host animals. Although a great majority of humans are infected with AAV2 during childhood, the sera of

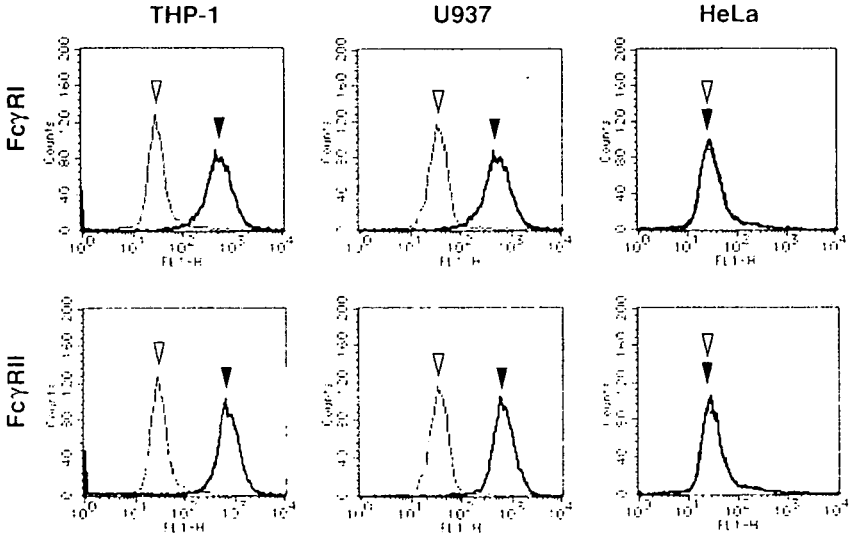

Fig. 6. Presence of Fcγ-RI and Fcγ-RII on THP-1 and U937 cells. THP-1, U937, and HeLa cells were incubated with anti-Fcγ-RI or anti-Fcγ-RII monoclonal antibodies followed by staining with the Alexa Fluor 488-conjugated goat anti-mouse IgG secondary antibody. The fluorescence on the cells was measured by using a flow cytometer. The bold line (indicated with filled arrowheads) shows the distribution of the resultant fluorescence. The thin line (indicated with open arrowheads) shows the distribution of the fluorescence of the cells incubated with only the secondary antibody.

Please cite this article as: Mori, S., et al., Antibody-dependent enhancement of adeno-associated virus infection of human monocytic cell lines, Virology (2008), doi:10.1016/j.virol.2008.01.033

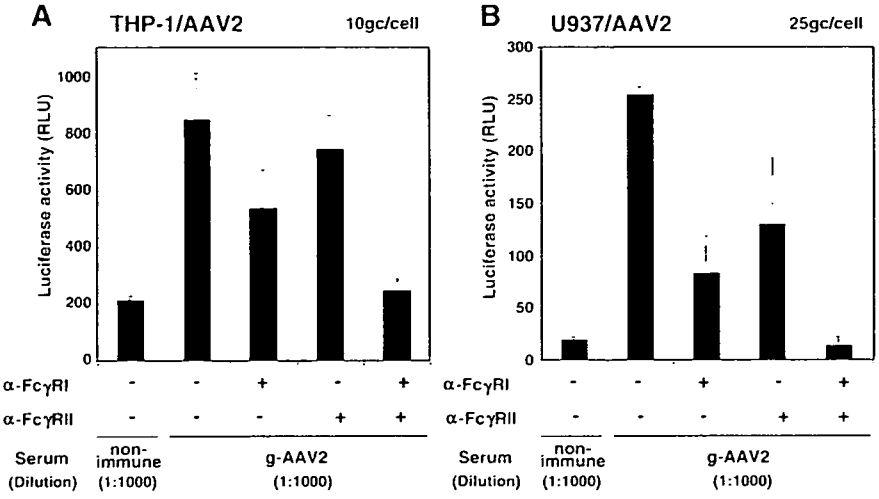

Fig. 7. Inhibition of ADE of AAV2 infection with anti-Fcγ-RI and anti-Fcγ-RII antibodies. THP-1 (A) and U937 (B) cells were pre-incubated with anti-Fcγ-RI and/or anti-Fcγ-RII mAbs. Then, AA2/Luc that had been incubated with anti-AAV2 antiserum was inoculated to the cells. Two days later, the luciferase activity of the cellular lysate was measured. Each bar represents the average of three independent experiments with the standard deviation indicated by an error bar. RLU: relative light units.

humans aged over 30 are positive for anti-AAV2 IgG and IgM antibodies simultaneously, indicating anti-AAV2 antibody induced by the primary infection does not protect the hosts from the secondary infection (Erles et al., 1999). Among human sera positive for anti-AAV antibody, only 30% of the sera are neutralizing (Chirmule et al., 1999). The level of anti-AAV antibody in the serum of the host persistently infected with AAV could be appropriate for the enhancement of AAV infection. Indeed the undiluted monkey-B sera, whose level of neutralizing antibody was below the detectable level, enhanced infection of THP-1 with AAV2/Luc (Fig. 5).

ADE is probably important for AAV to be maintained in host animals. Because the chance for the AAV-infected cell to be super-infected with the helper virus must be very rare in vivo, AAV may survive with a low level autonomous propagation induced by the Fas-mediated apoptosis of the host cell (Mori et al., 2002). ADE may support infection of a new host cell, mainly a leukocyte, with AAV.

Previous studies have shown that the capability of an antibody to contribute to ADE is independent of neutralizing activity. The monoclonal neutralizing antibodies against West Nile virus and against Dengue virus (Pierson et al., 2007; Yamanaka et al., 2008) and non-neutralizing antibodies against human respiratory syncytial virus (Gimenez et al., 1996) enhance infection of FcR bearing cells with these viruses, respectively. It is necessary to examine a panel of anti-AAV monoclonal antibodies for their capability of contributing to ADE and for their binding characteristics to AAV particles in future studies.

ADE may be useful for ex vivo immunotherapy, which uses antigen-presenting cells transduced with AAV vectors in vitro (Ponnazhagan et al., 2001; Veron et al., 2005). Because the antigen-presenting cells, such as monocytes and dendritic cells, are positive for Fcγ-RI and Fcγ-RII, pre-incubation of the AAV vectors with anti-AAV antibodies at a sub-neutralizing level, would increase the efficiency of transduction.

This is the first report showing the ADE of infection of Fcγ-R-bearing cells with the dependovirus. ADE has been observed in infection of Fcγ-R-bearing cells with the autonomous parvoviruses, such as human parvovirus B19 (Munakata et al., 2006) and Aleutian mink disease parvovirus (Kanno et al., 1993). The Fcγ-R-mediated ADE of infection may be common to those belonging to *Parvoviridae*.

Experimental Procedures

Cells

THP-1 and U937, human monocytic cell lines, were purchased from American Type Culture Collection (Manassas, VA). THP-1 was cultured in RPMI 1640 medium supplemented with 10% fetal bovine serum (FBS) and 50 μM 2-β-mercaptoethanol at 37 °C. U937 was cultured in RPMI 1640 medium supplemented with 10% FBS at 37 °C. HeLa cells that had been adapted to the suspension condition were cultured in suspension minimal essential medium (S-MEM) supplemented with 10% FBS with gentle shaking at 37 °C.

AAV vectors

A vector plasmid pAAVLuc was packaged into the AAV2 and AAV10 capsids to produce AAV2/Luc and AAV10/Luc, respectively, in HEK293 cells as described previously (Mori et al., 2004). The pAAVLuc is composed of the 5′-inverted terminal repeats (ITR) of AAV2, simian virus 40 early enhancer/promoter, firefly luciferase gene, and 3′-ITR. AAV2/Luc and AAV10/Luc were purified by heparin affinity column chromatography (Auricchio et al., 2001) and CsCl equilibrium centrifugation (Mori et al., 2004), respectively. Genome copy numbers of the vector stocks were measured by real-time PCR with TaqMan probes for the firefly luciferase gene (Perkin-Elmer Biosystems, Foster City, CA).

Please cite this article as: Mori, S., et al., Antibody-dependent enhancement of adeno-associated virus infection of human monocytic cell lines, Virology (2008), doi:10.1016/j.virol.2008.01.033

Antisera

Anti-AAV2 antiserum was obtained by an intramuscular injection of purified AAV2 vector having β-galactosidase gene (10^9 genome copies per mouse) to eight-week-old female BALB/c mice. The serum was collected at 6 weeks after the injection. Mouse anti-AAV10 serum was produced previously by immunizing mice with VP2, one of three capsid proteins (Mori et al., 2004). Mouse anti-CD64 and anti-CD32 monoclonal antibodies (BD Bioscience PharMingen, San Diego, CA) were used in the detection and blocking of Fcγ-RI and Fcγ-RII, respectively.

Monkey sera

Sera were obtained from two cynomolgus monkeys kept in Tsukuba Primate Research Center, National Institute of Biomedical Innovation. The monkeys were sedated during collection of blood by administration of Ketamine (10 mg/kg). Animal studies were performed in accordance with the guidelines for animal experiments in the National Institute of Infectious Diseases.

Assay for AAV infection

AAV vectors were suspended in phosphate-buffered saline (PBS) containing 5% FBS. 15 μl of vector suspension was mixed with an equal volume of the test serum that had been heat-inactivated (56 °C for 30 min) and diluted with PBS, and incubated at 37 °C for 30 min. The mixture was inoculated to 3×10^5 cells in a microtube. After incubation at 4 °C for 1 h with occasional rocking, the cells were washed with culture medium twice and resuspended in 780 μl of culture medium. The cell-suspension was seeded in 3 wells (250 μl/well) of a 48-well culture plate and incubated at 37 °C for 2 days. The cells were harvested and lysed. Luciferase activity of the lysate was measured by using Luciferase Assay System (Promega, Madison,WI) and Mithras LB940 Multilabelreader (Berthold Technologies, Bad Wildbad, Germany).

Flow cytometry

THP-1, U937, and HeLa cells were incubated with 2.5 μg/ml of anti-CD64 or anti-CD32 monoclonal antibody in reaction buffer (PBS containing 2% FBS) for 1 h at 4 °C. The cells were washed with the buffer twice and incubated in the buffer containing 2.5 μg/ml of Alexa Fluor 488-conjugated goat anti-mouse IgG serum (Molecular Probes, Eugene, OR). The cells were washed twice with the buffer and then fixed with 2% paraformaldehyde in PBS. Fluorescence was measured using a flow cytometer (BD FACSCalibur, Becton Dickinson, Franklin Lakes, NJ).

Blocking of FcγR on THP-1 and U937 cells

THP-1 and U937 cells were incubated with the culture medium containing 5 μg/ml of anti-CD64 (BD Bioscience PharMingen) and/or anti-CD32 (BD Bioscience PharMingen) at 4 °C for 1 h. The cells were washed twice with the culture medium and used in the assay for AAV infection.

Acknowledgments

We thank Dr. Kunito Yoshiike for critical reading of the manuscript. This work was supported by a grant-in-aid from the Ministry of Health, Labour and Welfare for the Third-Term Comprehensive 10-year Strategy for Cancer Control.

References

Auricchio, A., Hildinger, M., O'Connor, E., Gao, G.P., Wilson, J.M., 2001. Isolation of highly infectious and pure adeno-associated virus type 2 vectors with a single-step gravity-flow column. Hum. Gene Ther. 12, 71–76.

Buller, R.M., Janik, J.E., Sebring, E.D., Rose, J.A., 1981. Herpes simplex virus types 1 and 2 completely help adenovirus-associated virus replication. J. Virol. 40, 241–247.

Carter, B.J., Laughlin, C.A., de la Maza, L.M., Myers, M., 1979. Adeno-associated virus autointerference. Virology 92, 449–462.

Cheung, A.K., Hoggan, M.D., Hauswirth, W.W., Berns, K.I., 1980. Integration of the adeno-associated virus genome into cellular DNA in latently infected human Detroit 6 cells. J. Virol. 33, 739–748.

Chirmule, N., Propert, K., Magosin, S., Qian, Y., Qian, R., Wilson, J., 1999. Immune responses to adenovirus and adeno-associated virus in humans. Gene Ther. 6, 1574–1583.

Clyde, K., Kyle, J.L., Harris, E., 2006. Recent advances in deciphering viral and host determinants of dengue virus replication and pathogenesis. J. Virol. 80, 11418–11431.

Cohen-Solal, J.F., Cassard, L., Fridman, W.H., Sautes-Fridman, C., 2004. Fcγ receptors. Immunol. Lett. 92, 199–205.

Conrad, C.K., Allen, S.S., Afione, S.A., Reynolds, T.C., Beck, S.E., Fee-Maki, M., Barrazza-Ortiz, X., Adams, R., Askin, F.B., Carter, B.J., Guggino, W.B., Flotte, T.R., 1996. Safety of single-dose administration of an adeno-associated virus (AAV)-CFTR vector in the primate lung. Gene Ther. 3, 658–668.

Davidoff, A.M., Gray, J.T., Ng, C.Y., Zhang, Y., Zhou, J., Spence, Y., Bakar, Y., Nathwani, A.C., 2005. Comparison of the ability of adeno-associated viral vectors pseudotyped with serotype 2, 5, and 8 capsid proteins to mediate efficient transduction of the liver in murine and nonhuman primate models. Molec. Ther. 11, 875–888.

Erles, K., Sebokova, P., Schlehofer, J.R., 1999. Update on the prevalence of serum antibodies (IgG and IgM) to adeno-associated virus (AAV). J. Med. Virol. 59, 406–411.

Favre, D., Provost, N., Blouin, V., Blancho, G., Cherel, Y., Salvetti, A., Moullier, P., 2001. Immediate and long-term safety of recombinant adeno-associated virus injection into the nonhuman primate muscle. Molec. Ther. 4, 559–566.

Flotte, T.R., Berns, K.I., 2005. Adeno-associated virus: a ubiquitous commensal of mammals. Hum. Gene Ther. 16, 401–407.

Gimenez, H.B., Chisholm, S., Dornan, J., Cash, P., 1996. Neutralizing and enhancing activities of human respiratory syncytial virus-specific antibodies. Clin. Diagn. Lab. Immunol. 3, 280–286.

Handa, H., Shiroki, K., Shimojo, H., 1977. Establishment and characterization of KB cell lines latently infected with adeno-associated virus type 1. Virology 82, 84–92.

Kanno, H., Wolfinbarger, J.B., Bloom, M.E., 1993. Aleutian mink disease parvovirus infection of mink macrophages and human macrophage cell line U937: demonstration of antibody-dependent enhancement of infection. J. Virol. 7, 7017–7024.

Lai, L., Davison, B.B., Veazey, R.S., Fisher, K.J., Baskin, G.B., 2002. A preliminary evaluation of recombinant adeno-associated virus biodistribution in rhesus monkeys after intrahepatic inoculation in utero. Hum. Gene Ther. 13, 2027–2039.

McPherson, R.A., Rosenthal, L.J., Rose, J.A., 1985. Human cytomegalovirus completely helps adeno-associated virus replication. Virology 147, 217–222.

Please cite this article as: Mori, S., et al., Antibody-dependent enhancement of adeno-associated virus infection of human monocytic cell lines. Virology (2008), doi:10.1016/j.virol.2008.01.033

Mori, S., Murakami, M., Takeuchi, T., Kozuka, T., Kanda, T., 2002. Rescue of AAV by antibody-induced Fas-mediated apoptosis from viral DNA integrated in HeLa chromosome. Virology 15, 90–98.

Mori, S., Wang, L., Takeuchi, T., Kanda, T., 2004. Two novel adeno-associated viruses from cynomolgus monkey: pseudotyping characterization of capsid protein. Virology 330, 375–383.

Mori, S., Takeuchi, T., Enomoto, Y., Kondo, K., Sato, K., Ono, F., Iwata, N., Sata, T., Kanda, T., 2006. Biodistribution of a low dose of intravenously administered AAV-2, 10, and 11 vectors to cynomolgus monkeys. Jpn. J. Infect. Dis. 59, 285–293.

Mori, S., Takeuchi, T., Enomoto, Y., Kondo, K., Sato, K., Ono, F., Sata, T., Kanda, T., 2008. Tissue distribution of cynomolgus adeno-associated viruses AAV10, AAV11, and AAVcy.7 in naturally infected monkeys. Arch. Virol. 153, 375–380.

Munakata, Y., Kato, I., Saito, T., Kodera, T., Ishii, K.K., Sasaki, T., 2006. Human parvovirus B19 infection of monocytic cell line U937 and antibody-dependent enhancement. Virology 345, 251–257.

Nathwani, A.C., Davidoff, A.M., Hanawa, H., Hu, Y., Hoffer, F.A., Nikanorov, A., Slaughter, C., Ng, C.Y., Zhou, J., Lozier, J.N., Mandrell, T.D., Vanin, E.F., Nienhuis, A.W., 2002. Sustained high-level expression of human factor IX (hFIX) after liver-targeted delivery of recombinant adeno-associated virus encoding the hFIX gene in rhesus macaques. Blood 100, 1662–1669.

Peiris, J.S., Porterfield, J.S., 1979. Antibody-mediated enhancement of flavivirus replication in macrophage-like cell lines. Nature 282, 509–511.

Peiris, J.S., Gordon, S., Unkeless, J.C., Porterfield, J.S., 1981. Monoclonal anti-Fc receptor IgG blocks antibody enhancement of viral replication in macrophages. Nature 289, 189–191.

Pierson, T.C., Xu, Q., Nelson, S., Oliphant, T., Nybakken, G.E., Fremont, D.H., Diamond, M.S., 2007. The stoichiometry of antibody-mediated neutralization and enhancement of West Nile virus infection. Cell Host Microbe. 1, 135–145.

Ponnazhagan, S., Mahendra, G., Curiel, D.T., Shaw, D.R., 2001. Adeno-associated virus type 2-mediated transduction of human monocyte-derived dendritic cells: implications for ex vivo immunotherapy. J. Virol. 75, 9493–9501.

Richardson, W.D., Westphal, H., 1981. A cascade of adenovirus early functions is required for expression of adeno-associated virus. Cell 27, 133–141.

Veron, P., Allo, V., Riviere, C., Bernard, J., Douar, A.M., Masurier, C., 2007. Major subsets of human dendritic cells are efficiently transduced by self-complementary adeno-associated virus vectors 1 and 2. J. Virol. 81, 5385–5394.

Wu, Z., Asokan, A., Samulski, R.J., 2006. Adeno-associated virus serotypes: vector toolkit for human gene therapy. Molec. Ther. 14, 316–327.

Yamanaka, A., Kosugi, S., Konishi, E., 2008. Infection-enhancing and -neutralizing activities of mouse monoclonal antibodies against dengue type 2 and 4 viruses are controlled by complement levels. J. Virol. 82, 927–937.

Please cite this article as: Mori, S., et al., Antibody-dependent enhancement of adeno-associated virus infection of human monocytic cell lines, Virology (2008), doi:10.1016/j.virol.2008.01.033

Arch Virol (2008) 153: 375–380
DOI 10.1007/s00705-007-1097-8
Printed in The Netherlands

Archives of Virology

Brief Report

Tissue distribution of cynomolgus adeno-associated viruses AAV10, AAV11, and AAVcy.7 in naturally infected monkeys

S. Mori[1], T. Takeuchi[1], Y. Enomoto[1], K. Kondo[1], K. Sato[1], F. Ono[2], T. Sata[3], T. Kanda[1]

[1] Center for Pathogen Genomics, National Institute of Infectious Diseases, Toyama, Shinjuku-ku, Tokyo, Japan
[2] Corporation for Production and Research of Laboratory Primates, Hachimandai, Tsukuba, Ibaraki, Japan
[3] Department of Pathology, National Institute of Infectious Diseases, Toyama, Shinjuku-ku, Tokyo, Japan

Received 20 August 2007; Accepted 29 October 2007; Published online 10 December 2007

Summary

Adeno-associated virus (AAV) is used in gene-therapy studies, but its tissue distribution is unknown in natural infection. We examined cynomolgus AAVs (previously isolated AAV10 and AAV11 and novel AAVcy.7) for their tissue distribution in 14 cynomolgi by type-specific PCR. We found AAV10, AAV11, and AAVcy.7 in 6, 10, and 14 monkeys, respectively, and two or three types in 11 monkeys, showing that these AAVs are widespread in the monkeys. We detected AAV at a higher level mainly in the lymphatic tissues and ileum, which suggests that AAV may invade the host through Peyer's patches in the ileum and infect immune cells.

*

Adeno-associated virus (AAV), a member of the genus *Dependovirus* of the family *Parvoviridae*, is a nonenveloped icosahedral particle with a genome of 4.7 kb single-stranded linear DNA. Pathogenicity of AAV has not been reported. The AAV genome has the rep and cap genes that encode the nonstructural Rep proteins and the capsid proteins (VP1, VP2 and VP3), respectively. The initial studies of AAV type 2 (AAV2) have shown that, upon infection of cultured human cells, the viral genome is integrated into chromosome 19 and is maintained as a latent provirus unless the cells are co-infected with a helper virus, such as adenovirus [8].

Recently Gao et al. [3, 4] have obtained various AAV DNAs from human and nonhuman primate tissue samples by PCR amplifying the signature region, which has a highly type-specific nucleotide sequence, with consensus primers that hybridize to the conserved region in the capsid gene. AAV DNA was detected in the heart, lung, liver, spleen, duodenum, kidney, and lymph node of rhesus monkeys. By using a similar PCR strategy, Mori et al. [6] newly detected AAV10 and AAV11 in DNA samples from cynomolgus monkeys, and Chen et al. [1] detected AAV DNA in the tonsil, lung, and spleen of children. These findings indicate that many AAVs, including unidentified ones, are widely disseminated throughout multiple tissues of humans and nonhuman primates [4]. To date we have only a limited knowledge of the AAV life cycle, such as the portal of entry, the role of helper viruses in

Correspondence: Tadahito Kanda, Department of Pathology, National Institute of Infectious Diseases, 1-23-1 Toyama, Shinjuku-ku, Tokyo 162-8640, Japan
e-mail: kanda@nih.go.jp

primary infection, sites of replication and latency, and molecular forms of viral DNA.

Recombinant AAV has been studied for its potential use as a gene-transfer vector in gene therapy. It has been indicated that pseudotyped vectors, which are the AAV2 vector genome packaged in the capsids of AAVs other than AAV2, transduced various tissues with different efficiency. For example, AAV1-pseudotype transduced mouse muscle efficiently by the injection of the vector into the muscle, and AAV8-pseudotype transduced mouse liver efficiently by the injection of the vector into the portal vein [2]. These findings suggest that each AAV type has its own tissue preference. However, the tissue tropism of AAV in the natural host has not been studied extensively. In this study, we examined three cynomolgus monkey AAVs for their tissue distribution in the naturally infected host.

Fourteen cynomolgus monkeys (4 to 5 years of age and weighing 3 to 5 kg), numbered from #1 to #14, were obtained from Tsukuba Primate Research Center, National Institute of Biomedical Innovation. All the animal studies were conducted in accordance with the guidelines for animal experiments at the National Institute of Infectious Diseases. Twelve monkeys (#1 to #4 and #6 to #13) had been intravenously injected with a AAV2 vector containing a beta-galactosidase gene or EGFP-tubulin fusion gene in the previous study [7]. The entire coding regions of AAV10 (GenBank accession number: AY631965) and AAV11 (AY631966) had been isolated from the ileum of monkey #4 and the liver of monkey #5, respectively, as described previously [6]. Animal tissues were harvested at necropsy and stored at −80 °C until use. DNA was extracted from approximately 25 mg of each frozen tissue by using a QIAamp DNA extraction kit (Qiagen GmbH, Hilden, Germany). The quality and quantity of DNA in the samples were verified by amplifying a part of the cellular G3PDH gene as described previously [7].

We found a novel AAV sequence in monkey #12. The DNA samples extracted from the spleen and ileum were examined by PCR with the consensus primers CP1 and CP5 (Fig. 1A), whose nucleotide sequences are highly conserved in the cap genes of

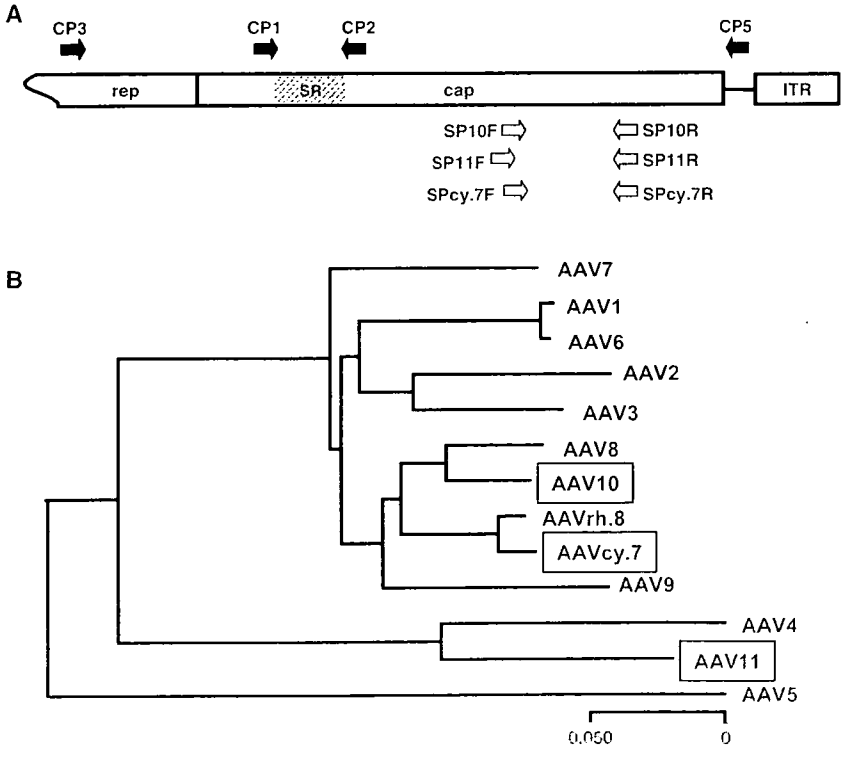

Fig. 1. Schematic representation of the AAV cap gene and phylogenetic tree of AAVs. (A) The signature region of AAV capsid gene and the PCR primers are indicated. (B) Phylogenetic tree based on the amino acid sequences of the capsid proteins. AAV types analysed in this study are indicated by boxes

the eleven AAV types, from AAV1 to AAV11 (6). Although AAV DNA was not amplified with the spleen sample, a DNA fragment of approximately 1.6 kilobase pairs (bp) was obtained from the ileum sample. The nucleotide sequence of the amplified fragment did not match those of any reported AAVs.

The entire coding region of the cap gene of the novel AAV was obtained by two sets of PCR using the DNA sample extracted from the ileum of monkey #12 and the consensus primers [6] (Fig. 1A). The 5′ region was amplified by using CP3 and CP2, and the 3′ region was amplified by using CP1 and CP5. The amino acid (aa) sequence deduced from the nucleotide sequence did not match those of any known AAVs. Therefore, we named the novel AAV AAVcy.7. The aa sequence of AAVcy.7 was similar to that of AAVrh.8 (97% homology), which had been obtained from a rhesus monkey [4]. The phylogenetic tree based on aa sequences of capsid protein is presented in Fig. 1B.

We attempted to detect the presence of AAV10, AAV11, and AAVcy.7 in the DNA samples of the various tissues of the monkeys by the PCR-amplification with primers specific for one of these types (Fig. 1A). The nucleotide sequences of the type-specific primers are as follows: forward primer for AAV10 (SP10F), 5′-GGGCCTGCAAACATGT CGGC; reverse primer for AAV10 (SP10R), 5′-CTGTTGACATTTCCCACAAT; SP11F, 5′-CTG AATCAAGGCAATGCAGC; SP11R, 5′-GCAGTC ACGTTGCCGGTTAT; SPcy.7F, 5′-GGGCCCAGC ACTATGGCCAA; SPcy.7R, 5′-TTGTGAACAAG TCCAGTCTG. These primer sets have been designed to amplify fragments of 395, 446, and 395 bp from AAV10, AAV11, and AAVcy.7 DNA, respectively. These primer sets amplified the target AAV DNA in the test samples containing AAV2, AAV4, AAV5, AAV8, AAV10, AAV11, or AAVcy.7 without non-specific amplification (data not shown). The level of the amplified DNA was estimated by the comparison of DNA amplified from the standard samples, which were a mixture of the cellular DNA extracted from African green monkey COS-1 cells (10^5 cells) and the plasmid DNA containing the AAV cap gene in the range from 10 to 10^5 copies, after ethidium bromide staining of the agarose gel. Approximately 10 copies of the cap gene in the standard sample were the minimum level of detection.

Nucleotide sequencing of the randomly selected PCR products showed that the detection and typing by the PCR with the type-specific primers was reliable. Seventeen PCR products obtained with the AAV10-specific primers and DNA samples of monkeys #3 and #5 were sequenced after cloning using pGEM-T vector system (Promega, Madison, WI). All of the DNA fragments were 395 nucleotides long. The aa sequences were deduced from the nucleotide sequences. The aa sequences of 4 clones were the same as with that of the registered AAV10. Ten clones had one aa replacement, R at aa 552 was replaced with K (AAV10/R552K), and 3 clones had one additional aa replacement (AAV10/R552K/S558I, AAV10/R552K/E577G, AAV10/R552K/D584N). Seven PCR products obtained with the AAV11-specific primers and DNA samples from monkeys #2 and #5 were sequenced. All of the DNA fragments were 446 nucleotides long. The aa sequence of one clone was same with that of the registered AAV11. One clone had one aa replacement (AAV11/Y490D), and 4 clones obtained from monkey #2 had two aa replacements (AAV11/V544I/N547T). Twenty PCR products obtained with the AAVcy.7-specific primers and DNA samples of monkeys #12 and #13 were sequenced. All of the DNA fragments were 395 nucleotides long. The aa sequences of 15 clones obtained from the cerebrum, spinal cord, ileum, and mesenteric lymph node of monkey #12 were identical to that of AAVcy.7. Five clones obtained from monkeys #13 had one aa replacement (AAVcy.7/A579S).

Table 1 shows the presence of AAV10, AAV11, and AAVcy.7 in the various tissues with the levels estimated by comparison to the standard samples. The blanks indicate that the samples were negative for the DNA amplification with the three sets of type-specific primers. AAV10, AAV11, and AAVcy.7 were detected in 6, 10, and 14 monkeys, respectively. Five monkeys (#1, #2, #5, #12, and #13) were infected with AAV10, AAV11, and AAVcy.7. Five monkeys (#3, #6, #7, #8, and #9) were infected with AAV11 and AAVcy.7. One monkey (#4) was infected with AAV11 and AAVcy.7. The data indicate that these AAVs are widespread in cynomolgus

Table 1. AAV10, 11, and cy.7 genomes in cynomolgus monkeys

	#1♀			#2♀			#3♀			#4♂			#5♀			#6♂			#7♀		
tissues	10	11	cy.7	10	11	cy.7	10	11	cy.7	10	11	cy.7	10	11	cy.7	10	11	cy.7	10	11	cy.7
cerebrum		+	+			+															
cerebellum																					
spinal cord	ND	ND	ND				ND	ND	ND	ND	ND	ND		+	+						
bone marrow										++		+	+	+++							
skin										ND	ND	ND									
eye			+											+	+						
muscle			+							ND	ND	ND									
bronchus																					
lung														++							
heart			+					+		+					+			++			
liver		+								+++				+++							+
gallbladder														+			+				
pancreas																					
spleen	+	++	+	+	+					++		+++	++	+++++						+	++
esophagus														+							
stomach										+		++		+							
jejunum				ND	ND	ND				++++			ND	ND	ND						++
ileum	+	+	+			+++				+++		+++		++++	+						
colon							ND	ND	ND					+							
kidney										+				+++							
adrenal gland		+								+			++	+++							
bladder										ND	ND	ND									
tonsil			+			+++			+++					+				+			
thymus													ND	ND	ND				ND	ND	ND
parotid gland																					
submandibular gland																					
thyroid gland														+							
axillary lymph node			+			+				++			+	+							
hilar lymph node	ND	ND	ND					+						+							+
mesenteric lymph node										ND	ND	ND	+	+++	+			+			++
iliac lymph node	ND	ND	ND			+	ND	ND	ND	ND	ND	ND		+							
inguinal lymph node	+		+							+			+	++				+			
testis/ovary																					
epididymis/uterus	ND	ND	ND															++			

	#8♂			#9♀			#10♀			#11♀			#12♂			#13♂			#14♀		
tissues	10	11	cy.7	10	11	cy.7	10	11	cy.7	10	11	cy.7	10	11	cy.7	10	11	cy.7	10	11	cy.7
cerebrum															+						
cerebellum																					
spinal cord															+						
bone marrow																					
skin																					
eye																					
muscle																					
bronchus																					
lung																					
heart					++							+									
liver																					
gallbladder						+															
pancreas													+								
spleen									+			+									+
esophagus			++																		
stomach			++									+									
jejunum									+												
ileum															+			+			
colon						++															
kidney																					
adrenal gland																					
bladder																					
tonsil														+							
thymus			++																		
parotid gland			+																		
submandibular gland																					
thyroid gland			+																		
axillary lymph node																+	+	+			+
hilar lymph node							ND	ND	ND	ND	ND	ND	ND	ND	ND	ND	ND	ND	ND	ND	ND
mesenteric lymph node															+						
iliac lymph node		+																	ND	ND	ND
inguinal lymph node						+								+							
testis/ovary			+																		
epididymis/uterus																					

10 AAV10, *11* AAV11, *cy.7* AAVcy.7.
+ $10–10^2$, ++ $10^2–10^3$, +++ $10^3–10^4$, ++++ $10^4–10^5$, +++++ 10^5 < genome copies/500 ng DNA.
ND Not done.

Table 2. Frequency of AAV genome detection in the tissues of cynomolgus monkeys

Tissues	AAV10			AAV11			AAVcy.7		
	Number of monkeys		Frequency	Number of monkeys		Frequency	Number of monkeys		Frequency
	A	B	A/B (%)	A	B	A/B (%)	A	B	A/B (%)
Cerebrum	0	6	0	1	10	10	3	14	21
Cerebellum	0	6	0	0	10	0	0	14	0
Spinal cord	0	4	0	1	8	13	2	11	18
Bone marrow	2	6	33	1	10	10	1	14	7
Skin	0	5	0	0	10	0	0	13	0
Eye	0	6	0	1	10	10	2	14	14
Muscle	0	5	0	0	10	0	1	13	8
Bronchus	0	6	0	0	10	0	0	14	0
Lung	0	6	0	1	10	10	0	14	0
Heart	1	6	17	2	10	20	4	14	29
Liver	1	6	17	2	10	20	1	14	7
Gallbladder	0	6	0	2	10	20	1	14	7
Pancreas	1	6	17	0	10	0	0	14	0
Spleen	4	6	67	4	10	40	6	14	43
Esophagus	0	6	0	1	10	10	1	14	7
Stomach	1	6	17	1	10	10	3	14	21
Jejunum	1	4	25	0	8	0	2	12	17
Ileum	2	6	33	2	10	20	6	14	43
Colon	0	6	0	1	9	11	1	13	8
Kidney	1	6	17	1	10	10	0	14	0
Adrenal gland	2	6	33	2	10	20	0	14	0
Bladder	0	5	0	0	10	0	0	13	0
Tonsil	0	6	0	2	10	20	4	14	29
Thymus	0	5	0	0	8	0	1	12	8
Parotid gland	0	6	0	0	10	0	1	14	7
Submandibular gland	0	6	0	0	10	0	0	14	0
Thyroid gland	0	6	0	1	10	10	1	14	7
Axillary lymph node	3	6	50	2	10	20	4	14	29
Hilar lymph node	0	3	0	2	7	29	1	8	13
Mesenteric lymph node	1	5	20	1	10	10	4	13	31
Iliac lymph node	0	4	0	2	8	25	1	10	10
Inguinal lymph node	3	6	50	2	10	20	3	14	21
Testis	0	3	0	0	4	0	1	5	20
Ovary	0	3	0	0	6	0	0	9	0
Epididymis	0	3	0	0	4	0	1	5	20
Uterus	0	2	0	0	5	0	0	7	0

A The number of the monkeys whose indicated tissue was positive for AAV DNA.
B The number of the monkeys with AAV-positive tissue(s) and whose indicated tissue was available for the test.

monkeys and that monkeys are commonly infected with multiple types of AAV.

Table 2 shows the frequency of the AAV DNA detection in the various tissues of monkeys having one or more tissues positive for the AAV DNA. Regardless of the types, these AAVs were frequently detected in the lymphoid tissues, such as the spleen and lymph nodes, as previously reported [3, 4], and in the ileum. The AAV10, AAV11, and AAVcy.7 were detected in the ileum of 33%, 20%, and 43% of the monkeys infected with AAV10, AAV11 and AAVcy.7, respectively, suggesting that AAV may invade the host through Peyer's patches in the ileum and infect immune cells, such as lymphocytes and macrophages, as many other pathogens do [5]. AAV10 and AAV11 were detected in

the kidney and adrenal gland less frequently, whereas AAVcy.7 was not detected in those tissues. Although AAV10 was not detected in the central nervous system (CNS), such as cerebrum and spinal cord, AAV11 and AAVcy.7 were detected in the CNS of two (#1 and #5) and four monkeys (#1, #2, #5, and #12), respectively. These results provide useful information for designing pseudotyped AAV vectors targeting the kidney or CNS.

Acknowledgements

We thank Dr. Kunito Yoshiike for critical reading of the manuscript. This work was supported by a grant-in-aid from the Ministry of Health, Labour and Welfare for the Third-Term Comprehensive 10-year Strategy for Cancer Control.

References

1. Chen CL, Jensen RL, Schnepp BC, Connell MJ, Shell R, Sferra TJ, Bartlett JS, Clark KR, Johnson PR (2005) Molecular characterization of adeno-associated viruses infecting children. J Virol 79: 14781–14792
2. Gao GP, Alvira MR, Wang L, Calcedo R, Johnston J, Wilson JM (2002) Novel adeno-associated viruses from rhesus monkeys as vectors for human gene therapy. Proc Natl Acad Sci USA 99: 11854–11859
3. Gao G, Alvira MR, Somanathan S, Lu Y, Vandenberghe LH, Rux JJ, Calcedo R, Sanmiguel J, Abbas Z, Wilson JM (2003) Adeno-associated viruses undergo substantial evolution in primates during natural infections. Proc Natl Acad Sci USA 100: 6081–6086
4. Gao G, Vandenberghe LH, Alvira MR, Lu Y, Calcedo R, Zhou X, Wilson JM (2004) Clades of Adeno-associated viruses are widely disseminated in human tissues. J Virol 78: 6381–6388
5. Jones B, Pascopella L, Falkow S (1995) Entry of microbes into the host: using M cells to break the mucosal barrier. Curr Opin Immunol 7: 474–478
6. Mori S, Wang L, Takeuchi T, Kanda T (2004) Two novel adeno-associated viruses from cynomolgus monkey: pseudotyping characterization of capsid protein. Virology 330: 375–383
7. Mori S, Takeuchi T, Enomoto Y, Kondo K, Sato K, Ono F, Iwata N, Sata T, Kanda T (2006) Biodistribution of a low dose of intravenously administered AAV-2, 10, and 11 vectors to cynomolgus monkeys. Jpn J Infect Dis 59: 285–293
8. Muzyczka N, Berns I (2001) Parvoviridae: the viruses and their replication. In: Knipe DM, Howley PM (eds) Fields virology, vol. 2. Lippincott Williams & Wilkins, Philadelphia, pp 2327–2359

Jpn. J. Infect. Dis., 59, 285-293, 2006

Original Article

Biodistribution of a Low Dose of Intravenously Administered AAV-2, 10, and 11 Vectors to Cynomolgus Monkeys

Seiichiro Mori, Takamasa Takeuchi, Yutaka Enomoto, Kazunari Kondo, Kaori Sato, Fumiko Ono[1], Naoko Iwata[2], Tetsutaro Sata[2] and Tadahito Kanda*

Center for Pathogen Genomics and [2]Department of Pathology, National Institute of Infectious Diseases, Tokyo 162-8640, and
[1]Corporation for Production and Research of Laboratory Primates, Ibaraki 305-0843, Japan

(Received May 12, 2006. Accepted June 26, 2006)

SUMMARY: In gene therapy trials, adeno-associated virus (AAV) vectors are injected directly into target tissues such as muscle and liver. Direct injection can lead to the introduction of a low level of the vector into blood circulation. To determine the systemic effects of the vector released in the blood, we extensively examined the biodistribution of intravenously administered AAV serotype 2 (AAV2) vector in cynomolgus monkeys. Although the vector distribution pattern varied from monkey to monkey, the vector DNA was maintained in the various tissues beyond 7 months post-inoculation (pi). The vector DNA was detected in the lymphoid tissues, particularly in the spleen, more frequently and at a much higher level than in the other tissues tested (i.e., brain, lung, liver, heart, gallbladder, pancreas, colon, kidney, ovary, uterus, etc.). The expression of a transgene was detected in the lymph nodes at 3 months pi. The distribution of two pseudotyped vectors, AAV2/10 and AAV2/11, was similar to that of the AAV2 vector. The present results suggest that when introduced intravenously, the AAV vector DNA persists and may induce transgene expression in various monkey tissues. Thus, the possibility of inadvertent gene transfer to various non-target tissues should be considered in a gene therapy strategy with an AAV vector.

INTRODUCTION

Adeno-associated virus (AAV), a nonenveloped small DNA virus belonging to the genus *Dependovirus* of the family *Parvoviridae*, has been engineered for use as a gene-transfer vector in gene therapy (1). Expression of a transgene introduced into target cells by the AAV vector is expected to last for a long period of time. Fundamental methods of AAV vector production, purification, and quality control have been developed by using the human AAV serotype 2 (AAV2) vector as a model system (2). Pseudotyped AAV2 vectors, in which the AAV2 vector genomes are packaged with capsids from AAVs of the other serotypes, have recently been developed (3). Some of the pseudotypes have shown organ tropism that differs from that of the AAV2 vector (3).

The AAV vector genome, which encodes a transgene, is a single-stranded 4.7 kb DNA. At each end of the vector genome is a 145-base region (inverted terminal repeat [ITR]) containing the viral origin of DNA replication and the packaging signal (1). Since the vector genome lacks the viral rep gene, the product of which mediates viral DNA replication and integration of the viral DNA into the AAVS1 region in human chromosome 19, the vector DNA is not replicable and is randomly integrated into host cell chromosomes or is maintained as episomes of the circularized intermediates (4,5). The vector capsid, an icosahedral particle with a diameter of 25 nm, is composed of the AAV capsid proteins (VP1, VP2, and VP3).

Since AAV vectors are highly stable and can infect various organs, AAV vectors are considered to be suitable for in vivo administration. However, the direct injection of an AAV vector into the target tissue leads to the infection of distant non-target tissues with the vector via blood circulation in non-human primates (6-11). The AAV2 vector, when administered by instillation to the bronchial epithelium of rhesus monkeys, is distributed to the heart, liver, jejunum, kidney, lymph nodes, spleen, pancreas, and brain (6). The AAV2 vector, when injected into the liver of rhesus fetuses, is distributed to the lymph node, liver, skin, spleen, lung, and esophagus of human infants (8). The AAV2 vector, when injected into the muscle, is distributed to the liver and lymph nodes (7). Thus, detailed evaluation of vector biodistribution to various tissues is a necessary part of the assessment of the safety of the vector in the context of administering a gene therapy strategy with in vivo administration.

In this study, the biodistribution of intravenously injected AAV2 vectors and pseudotyped AAV2/10 and 2/11 vectors in cynomolgus monkeys was examined in more extensive detail than that of previous studies (6-11). These studies show that the entry of a portion of the vector into the blood vessels is unavoidable after direct inoculation of the vector into the target tissue. Given the doses of AAV vectors used in clinical trials (2×10^{12} genome copies [gc]/kg weight), we chose AAV vector doses of 2×10^{9} gc to 5×10^{10} gc/kg weight for intravenous injection into the monkeys, assuming that 1/100 to 1/1,000 of the inoculate could leak into the bloodstream from the tissue that had received the vector injection. The AAV vector DNA in the tissue samples was measured semi-quantitatively by agarose gel electrophoresis of a PCR-amplified vector DNA. The results were expected to provide basic data required to evaluate the safety of in vivo administration of the AAV vectors.

*Corresponding author: Mailing address: Center for Pathogen Genomics, National Institute of Infectious Diseases, Toyama 1-23-1, Shinjuku-ku, Tokyo 162-8640, Japan. Tel: +81-3-5285-1111 ext. 2524, Fax: +81-3-5285-1166, E-mail: kanda@nih.go.jp